Research Article Vol. 33, No. 11 / 2 Jun 2025 / Optics Express 22988
Optics EXPRESS

Diode-pumped mode-locked Yb:$Ca_3La_2(BO_3)_4$ laser generating 35 fs pulses

HUANG-JUN ZENG,[1] ZHANG-LANG LIN,[1] GE ZHANG,[1] ZHONGBEN PAN,[2] PAVEL LOIKO,[3] XAVIER MATEOS,[4] VALENTIN PETROV,[5] HAIFENG LIN,[6,7] AND WEIDONG CHEN[1,5,*]

[1]*State Key Laboratory of Functional Crystals and Devices, Fujian Institute of Research on the Structure of Matter, Chinese Academy of Sciences, 350002 Fuzhou, China*
[2]*School of Information Science and Engineering, Shandong University, 266237 Qingdao, China*
[3]*Centre de Recherche sur les Ions, les Matériaux et la Photonique (CIMAP), UMR 6252 CEA-CNRS-ENSICAEN, Université de Caen, 6 Boulevard Maréchal Juin, 14050 Caen Cedex 4, France*
[4]*Universitat Rovira i Virgili, URV, Física i Cristal·lografia de Materials (FiCMA), Marcel·lí Domingo 1, 43007 Tarragona, Spain*
[5]*Max Born Institute for Nonlinear Optics and Short Pulse Spectroscopy, Max-Born-Str. 2a, 12489 Berlin, Germany*
[6]*Department of Physics, Umeå University, 901 87 Umeå, Sweden*
[7]*haifeng.lin@umu.se*
[*]*chenweidong@fjirsm.ac.cn*

Abstract: We present a comprehensive study of both continuous-wave and first mode-locked operation of a diode-pumped Yb:$Ca_3La_2(BO_3)_4$ laser in the soliton regime. Using a 976-nm single-spatial-mode, fiber-coupled InGaAs diode laser as pump source, the Yb:$Ca_3La_2(BO_3)_4$ laser delivers a maximum continuous-wave output power of 491 mW at 1050.6 nm, with a slope efficiency of 63%. Passive mode-locking is realized using a commercial semiconductor saturable absorber mirror, generating soliton pulses as short as 35 fs at 1055.9 nm, with an average output power of 96 mW at a pulse repetition rate of ~66.5 MHz. By optimizing the output coupling, the average output is scaled to 239 mW for slightly longer 48-fs pulses at 1051.9 nm, corresponding to a peak power of 65.9 kW and a laser efficiency of 29%. These results highlight the potential of Yb:$Ca_3La_2(BO_3)_4$ as a gain medium for sub-50-fs ultrafast laser applications.

1. Introduction

In the past years, a significant progress has been demonstrated in the field of femtosecond mode-locked (ML) lasers operating at 1 μm based on ytterbium (Yb^{3+}) ions. The three key enabling technologies for the design of such sources are i) the saturable absorber, ii) the broadly emitting gain medium and iii) the intracavity dispersion management for soliton pulse shaping. GaAs/AlGaAs-based semiconductor saturable absorber mirrors (SESAMs) with reliable nonlinear characteristics are commercially available for 1-μm lasers. The most recent trend for cavity dispersion management includes the use of low-loss dispersive mirrors with a controlled number of bounces. In the material field, the search for Yb^{3+}-doped gain media is still ongoing, targeting a material combining i) spectrally broad, smooth and flat gain profiles supporting sub-50 fs pulse generation, ii) good thermal properties for average power scaling, iii) facile growth method and high optical quality of the crystals which is essential for transferring the technology towards industry, and iv) attractive nonlinear optical properties (*i.e.*, high nonlinear refractive index n_2 for SESAM assisted or pure Kerr lens mode-locking).

The control of the gain bandwidth can be enabled in several ways, namely i) by inducing a strong inhomogeneous spectral line broadening dominating the homogeneous (temperature) broadening via the use of disordered materials, ii) using combined gain media in a single cavity, or

#563483 https://doi.org/10.1364/OE.563483
Journal © 2025 Received 7 Apr 2025; revised 10 May 2025; accepted 10 May 2025; published 23 May 2025

Optics EXPRESS

iii) polarization multiplexing, *i.e.*, by combining spectral gain profiles from two eigen-polarization states of a single anisotropic crystal. The first approach holds great promise as a single laser gain crystal can be employed operated at a given polarization state corresponding to the broadest gain bandwidth. The disorder comprises the i) structure disorder (random cation site distribution), ii) compositional disorder (in "mixed" or solid-solution compounds), iii) crystals with rare-earth ion clustering, or a combination of the above-mentioned approaches. The inevitable weakness of disordered materials is the associated drop in thermal conductivity (even for undoped matrices, which is further enhanced upon doping with laser active ions, *e.g.*, Yb^{3+}) [1–3]. In this way, a compromise between the appealing spectroscopic and tolerated thermal properties needs to be reached.

Borate crystals are high phonon energy compounds which attract attention for doping with Yb^{3+} ions for applications in femtosecond ML lasers capable of generating sub-100 fs pulses in the spectral range of ~1 μm [4–6]. In the present work, we turn our attention to Yb^{3+}-doped rare-earth calcium borates with the chemical formula of Yb:$Ca_3Ln_2(BO_3)_4$ (where Ln^{3+} represents Gd^{3+} [7], Y^{3+} [8], or La^{3+} [9]). These crystals adopt an orthorhombic structure with the centrosymmetric space group *Pnma* (D_{2h}^{16}) and consist of isolated BO_3 triangles, along with Ln^{3+} - oxygen and calcium-oxygen polyhedrons [1,10]. They melt congruently at a relatively low temperature (~1400°C) and can be grown into large-volume boules using the Czochralski method [9]. The structure disorder in these borates originates from the random distribution of Ca^{2+} and $Ln^{3+}|Yb^{3+}$ cations over three non-equivalent crystallographic sites, leading to pronounced inhomogeneous spectral broadening arising from the multi-site nature of the crystal [11]. As a result, these materials exhibit "glassy-like" spectroscopic behavior but suffer from relatively low thermal conductivity (0.9 -1.04 W/mK at room temperature for the undoped Gd and Y compounds) [1]. To date, Yb:$Ca_3Ln_2(BO_3)_4$ crystals have been extensively studied for efficient lasers operating in both continuous-wave (CW) and ML regimes. For example, a diode-pumped CW Yb:$Ca_3Y_2(BO_3)_4$ laser delivered an output power of 1.17 W with a slope efficiency of 22.1% [12]. Using a SESAM, a diode-pumped ML Yb:$Ca_3Y_2(BO_3)_4$ laser generated 244 fs pulses at 1044.7 nm, with an average output power of 261 mW [13]. When pumped by a high-power, multi-transverse mode InGaAs laser diode at 976 nm, an Yb:$Ca_3Gd_2(BO_3)_4$ laser produced 5.58 W output power in CW operation, with a slope efficiency of 51.7% and a laser efficiency of 49.7% [14]. Moreover, soliton pulses as short as 39 fs were demonstrated from a diode-pumped SESAM ML Yb:$Ca_3Gd_2(BO_3)_4$ laser at 1059.2 nm, with an average output power of 70 mW [15].

Within isostructural families of laser crystals, a certain variation of the crystal-field strength and electron-phonon interaction both affecting the spectral gain profiles can be reached via an appropriate choice of the host-forming cation (Ln^{3+}, in our case) being substituted by the dopant ions (Yb^{3+}). It is often desirable to choose materials with a larger difference between the ionic radii of the host-forming and dopant ions, as this is expected to distort the multi-ligand around the active ion. Lanthanum-based crystals sound appropriate in this regard. Yb:$Ca_3La_2(BO_3)_4$ (abbreviated as Yb:LaCB) is another representative of the Yb:$Ca_3Ln_2(BO_3)_4$ crystal family. In its host lattice, Ca^{2+} and La^{3+} ions statistically occupy three non-equivalent crystallographic sites (M_1, M_2 and M_3). The crystal structure consists of three sets of Ca-oxygen distorted polyhedra (CaO_8) and three sets of isolated BO_3 planar triangles. When Yb^{3+} ions replace La^{3+} cations in all three M_1 – M_3 sites, they experience diverse multi-ligand environments, leading to pronounced inhomogeneous spectral line broadening [16]. As a result, Yb:LaCB features a "glassy-like" spectral response, featuring broad absorption and emission spectra at ~1 μm, as well as an extremely broad, flat, and smooth gain profile suitable for sub-100 fs pulse generation via passive mode-locking [16]. The primary drawback of this crystal is its relatively low thermal conductivity (0.4 - 0.6 $Wm^{-1}K^{-1}$ at room temperature for 4.32 at.% Yb doping), which stems from its disordered structure [17]. The laser performance of Yb:LaCB has been

Optics EXPRESS

investigated in both CW and Q-switched regimes [18,19]. When pumped by a high-power, multi-transverse-mode, fiber-coupled laser diode at 976 nm, a maximum output power of 8.2 W was achieved in the CW regime at 1043 nm, corresponding to a laser efficiency of 33% [16]. In the Q-switched regime, a Cr^{4+}:YAG saturable absorber enable the generation of pulses with a maximum average output power of 3 W at 1018.7 nm, a pulse duration of 5.3 ns, and a pulse repetition rate of 5 kHz [20]. However, to date, no passively ML laser operation using Yb:LaCB has been demonstrated.

In this study, we present a comprehensive investigation of both CW and passively ML regimes of a Yb:LaCB laser. Using a SESAM to initiate and stabilize mode-locking, sub-40 fs pulses are generated for the first time to the best of our knowledge.

2. Experimental setup

The experimental setup of the diode-pumped Yb:LaCB laser is shown in Fig. 1. The laser sample was cut from the as-grown crystal boule with a doping concentration of 4.32 at.% for light propagation along the ***a***-axis (***a***-cut). The sample had dimensions of 3.3 mm × 3.3 mm in aperture and 3 mm in thickness. It was polished to laser-grade quality with good parallelism and remained uncoated. The crystal was mounted in a copper holder without active cooling and positioned at Brewster's angle between two concave mirrors (labelled M_1 and M_2) with a radius of curvature (RoC) of -100 mm, forming an X-shaped astigmatically compensated linear cavity. The laser polarization was aligned along the crystallographic ***c***-axis (*i.e.*, $\boldsymbol{E} \parallel \boldsymbol{c}$). The pump source was a fiber-coupled InGaAs laser diode emitting unpolarized radiation at 976 nm, providing a maximum incident power of 1.29 W. The diode featured a nearly diffraction-limited beam quality of output radiation, with a beam propagation factor (M^2) of ~1.02. The emission wavelength was stabilized using a fiber Bragg gating (FBG), yielding a spectral linewidth (full width at the half maximum, FWHM) of ~0.2 nm. The pump beam was first collimated using an aspherical lens L_1 (focal length: $f = 26$ mm) and subsequently focused into the laser crystal through the M_1 mirror using an achromatic doublet lens L_2 ($f = 100$ mm). This optical configuration resulted in a focused beam waist (radius) of 18.9 μm × 37.9 μm in the sagittal and tangential planes, respectively.

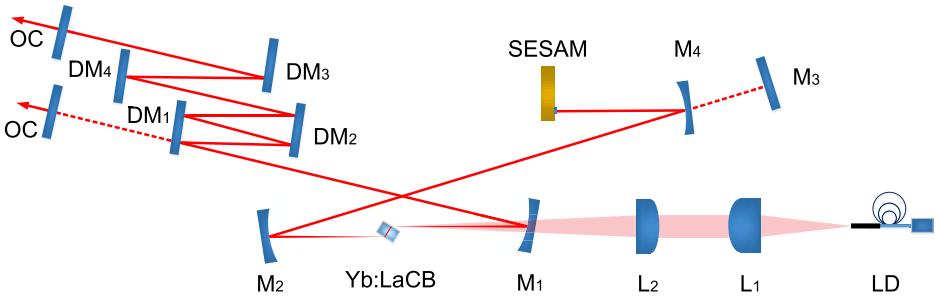

Fig. 1. Schematic of the diode-pumped Yb:LaCB laser. LD: fiber-coupled InGaAs laser diode; L_1: aspherical lens; L_2: achromatic doublet; M_1, M_2 and M_4: concave mirrors (RoC = -100 mm); M_3: flat end mirror for CW laser operation; DM_1 - DM_4: flat dispersive mirrors; OC: output coupler; SESAM: SEmiconductor Saturable Absorber Mirror.

The CW performance of the Yb:LaCB laser was studied using a four-mirror cavity without a SESAM or dispersive mirrors (DMs). One arm of the cavity was terminated by a flat end mirror M_3, while the other contained a plane-wedged output coupler (OC) with variable transmission (T_{OC}) ranging from 0.6% to 10%. The cavity mode radius inside the laser crystal was estimated using the ABCD matrix method, yielding values of 21 μm × 37 μm in the sagittal and tangential planes, respectively. Under lasing conditions, the measured pump absorption slightly decreased

Optics EXPRESS

from 67.3% to 62.2% as T_{OC} increased from 0.6% to 10%, which can be attributed to the reduced population recycling effect.

For ML operation, the flat end mirror M_3 was replaced with a third plane-concave mirror, M_4 (RoC = -100 mm), creating a secondary intracavity beam waist with a radius of ~80 μm at the SESAM to ensure efficient saturation. The SESAM, acting as the rear cavity reflector, was a commercial device (BATOP, GmbH) with the following specifications: a modulation depth of ~1.2% at ~1 μm, a non-saturable loss of ~0.8%, a saturation fluence of 60 μJ/cm^2, and a recovery time of ~1 ps. To manage the intracavity group delay dispersion (GDD), four flat DMs (DM_1 – DM_4) with different negative GDD values per bounce (DM_1 = -55 fs^2, DM_2 = -100 fs^2, $DM_3 = DM_4$ = -250 fs^2) were incorporated into the extended cavity arm. These mirrors compensated for material GDD and helped balance the self-phase modulation (SPM), enabling stable soliton-like pulse formation. The total round-trip negative GDD was -1620 fs^2. The geometric cavity length of the ML laser was ~2 m, corresponding to a pulse repetition rate of ~66.5 MHz.

3. Experimental results

3.1. Continuous-wave laser results

The CW laser performance of the Yb:LaCB crystal is shown in Fig. 2. Using a 2.5% OC, the laser emitted a maximum output power of 491 mW at an absorbed pump power of 867 mW, corresponding to the highest slope efficiency of 63% and a laser efficiency of 56.6%. The laser threshold exhibited a gradual increase with T_{OC}, rising from 50 mW for 0.6% OC to 137 mW for 10% OC. Moreover, as T_{OC} increased, the emission wavelength in the CW regime underwent a blue-shift from 1070.6 nm to 1033.1 nm, as illustrated in Fig. 2(b).

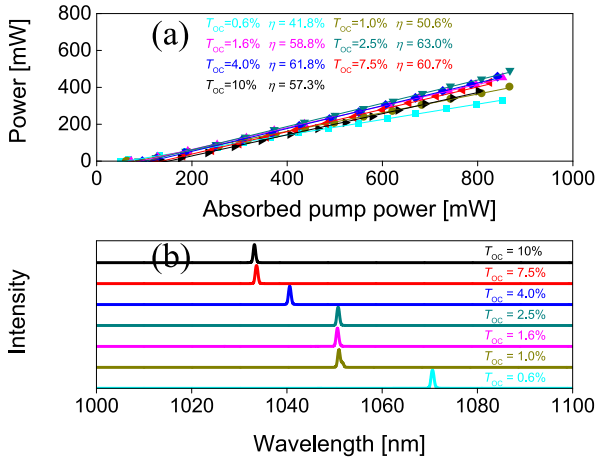

Fig. 2. CW diode-pumped Yb:LaCB laser: (a) Input-output dependences for different OCs, η – slope efficiency; (b) laser spectra.

To estimate the total round-trip cavity losses (δ, excluding reabsorption losses) and the intrinsic slope efficiency (η_0) – the Caird analysis [21] was applied. The measured slope efficiency was fitted as a function of the OC reflectivity ($R_{OC} = 1\text{-}T_{OC}$), yielding best-fit values of $\eta_0 = 68.4 \pm 2\%$ and $\delta = 0.3 \pm 0.03\%$, as shown in Fig. 3(a). The low value of δ indicates a well-optimized cavity alignment and a high-optical-quality laser crystal, despite the relatively large ionic radius difference of Yb and La. The wavelength tuning behavior of the Yb:LaCB laser in the CW regime was explored by inserting an SF10 prism at Brewster's angle near the OC ($T_{OC} = 0.4\%$).

Optics EXPRESS

The laser wavelength was found to be continuously tunable over 94 nm, from 999 to 1093 nm, as shown in Fig. 3(b).

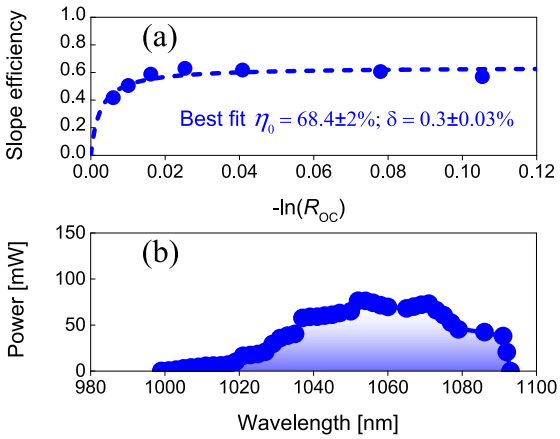

Fig. 3. CW diode-pumped Yb:LaCB laser: (a) Caird analysis for assessing the total round-trip cavity losses δ and intrinsic slope efficiency η_0; (b) wavelength tuning curve with a SF10 prism and a 0.4% OC. The output polarization is $\boldsymbol{E}\|\boldsymbol{c}$.

3.2. *Mode-locked laser results*

Initially, ML operation of the diode-pumped Yb:LaCB laser was studied with a 4% OC. Continuous-wave mode-locking (CW-ML) was readily achieved by careful cavity alignment.

Figure 4(a) depicts the measured optical spectrum of the laser pulses, which is centered at 1056.4 nm with a spectral width of 29.8 nm (FWHM), assuming a sech^2-shape. Under these conditions, the maximum average output power reached 201 mW for a pulse repetition rate of 66.5 MHz at an absorbed pump power of 842 mW. This performance represents a laser efficiency of 23.9% and a peak power of 64.9 kW. The recorded intensity autocorrelation trace based on second-harmonic generation (SHG) was well fitted by a sech^2-shaped temporal profile, yielding an estimated pulse duration of 41 fs, as shown in Fig. 4(b). The corresponding time-bandwidth product (TBP) was calculated to be 0.328, slightly above the Fourier-transform limit of 0.315. A long-scale autocorrelation scan over 50 ps, shown in the inset of Fig. 4(b), confirmed steady-state single-pulse CW-ML operation.

The shortest pulse duration was obtained by using a 1.6% OC while maintaining the same negative GDD. Figure 5 illustrates the measured optical spectrum and autocorrelation trace of these shortest pulses at a pulse repetition rate of 66.5 MHz. The spectrum was centered at 1055.9 nm with width of 34.6 nm, assuming a sech^2-shape, as seen in Fig. 5(a). The autocorrelation trace exhibited an excellent fit to a sech^2-shaped temporal profile, indicating a deconvolved pulse duration of 35 fs, as shown in Fig. 5(b). A long-term autocorrelation scan over 50 ps, depicted in the inset of Fig. 5(b), further confirmed stable single-pulse mode-locking. In this configuration, the average output power was dropped to 96 mW at an absorbed pump power of 853 mW, corresponding to a peak power of 36.3 kW. The calculated TBP of 0.326 again suggests a pulse duration slightly above the Fourier-limit. The ML operation producing the shortest pulses was not reliably self-starting; however, minor perturbations were sufficient to initiate mode-locking, which then remained stable once established.

The unreliable self-starting and the high brightness of the employed laser diode alone are not sufficient evidence for the prevailing role of Kerr-lens mode-locking (KLM) in the Yb:LaCB laser. To clarify this, we monitored the far-field beam profiles before and after initiating ML

Optics EXPRESS

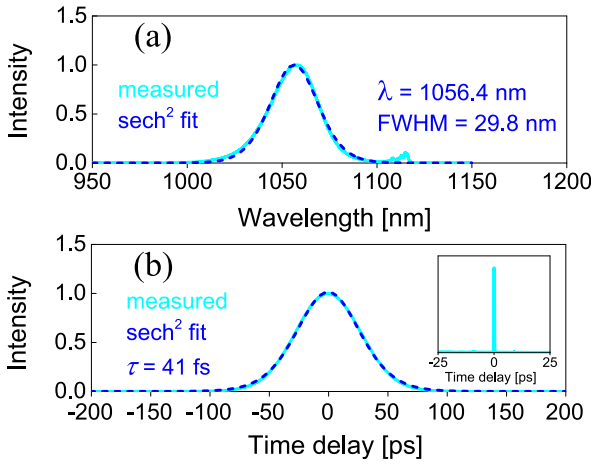

Fig. 4. Diode-pumped ML Yb:LaCB laser with $T_{OC} = 4\%$: (a) Optical spectrum (b) SHG-based intensity autocorrelation trace. *Inset*: autocorrelation trace on a time span of 50 ps.

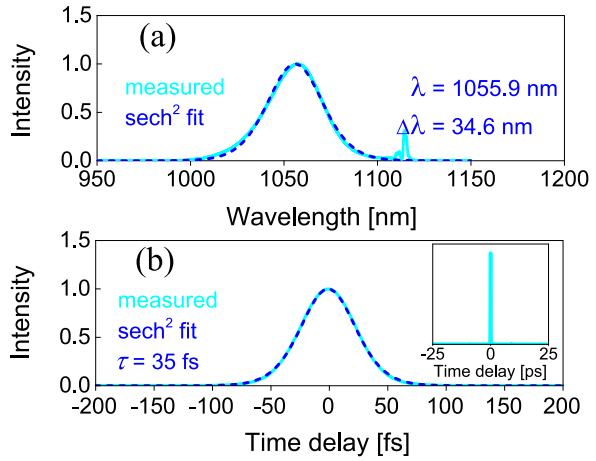

Fig. 5. Diode-pumped ML Yb:LaCB laser with a 1.6% OC: (a) Optical spectrum (b) SHG-based intensity autocorrelation trace. *Inset*: autocorrelation trace on a time span of 50 ps.

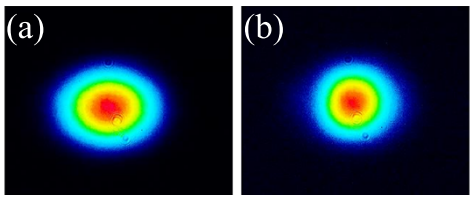

Fig. 6. Measured far-field beam profiles of the shortest pulses from the diode-pumped ML Yb:LaCB laser: (a) CW and (b) ML regimes of operation.

Optics EXPRESS

operation using an IR camera placed ~1.0 m from the OC, as shown in Fig. 6. The significant reduction of the beam diameters - from 2.22 mm (x) × 1.67 mm (y) in the CW regime to 1.72 mm (x) × 1.63 mm (y) in the ML regime confirmed that KLM, supported by the SESAM, was indeed the dominant ML mechanism.

Figure 7 presents the measured radio-frequency (RF) spectra for the shortest pulses at the first beat-note frequency of 66.5 MHz, recorded with a resolution bandwidth (RBW) of 300 Hz, alongside a broader 1-GHz frequency span measurement using a RBW of 100 kHz. The exceptionally high extinction ratio of 78 dBc above noise floor at the first beat-note frequency and the absence of any spurious modulation confirm the stable and clean CW-ML operation of the Yb:LaCB laser.

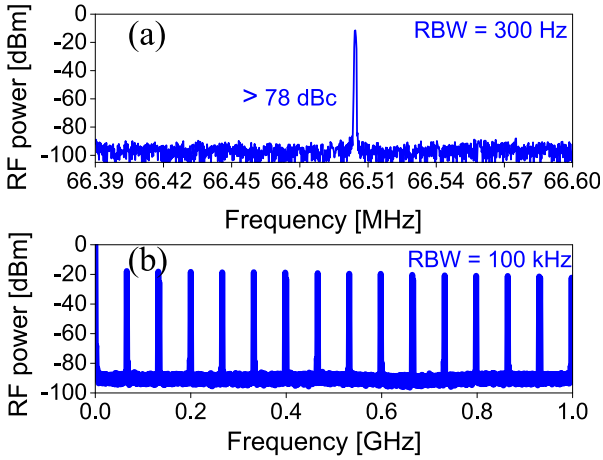

Fig. 7. RF spectra of the diode-pumped ML Yb:LaCB laser with 1.6% OC: (a) First beat note at 66.5 MHz recorded using a RBW of 300 Hz, and (b) harmonics on a 1-GHz frequency span recorded using a RBW = 100 kHz.

Power scaling of the diode-pumped ML Yb:LaCB laser was achieved using a 7.5% OC at a pulse repetition rate of 66.5 MHz. Under these conditions, the average output power reached 239 mW at an absorbed pump power of 825 mW, corresponding to a laser efficiency of 29%. For a somewhat longer pulse duration of 48 fs, the peak power reached 65.9 kW. The output characteristics of the diode-pumped ML Yb:LaCB laser achieved in this work are summarized in Table 1.

Table 1. Output Characteristics[a] of the Mode-Locked Yb:LaCB Laser

T_{OC}, %	P_{out}, mW	P_{abs}, mW	P_{peak}, kW	λ_{em}, nm	$\Delta\lambda_{em}$, nm	$\Delta\tau$, fs	TPB
1.6	96	853	36.3	1055.9	34.6	35	0.326
4	201	842	64.9	1056.4	29.8	41	0.328
7.5	239	825	65.9	1051.9	24.6	48	0.320

[a] T_{OC} – transmittance of the output coupler, P_{out} – average output power, P_{abs} – absorbed pump power, P_{peak} – peak power, λ_{em} – central emission wavelength, $\Delta\lambda_{em}$ – emission bandwidth (FWHM), $\Delta\tau$ – pulse duration (FWHM), TBP – time bandwidth product.

It is interesting to position the obtained mode-locked laser performance with those for other Yb^{3+}-doped borate crystals. In Fig. 8, we compare the pulse duration and the average output power for 1-μm lasers based on various borate crystals studied by us recently using a similar laser architecture including the cavity design, the SESAMs and the dispersion management. Both

Optics EXPRESS

the cases of SESAM mode-locking and Kerr-lens mode-locking are considered. One can see that the studied compound, Yb:LaCB, provides a good compromise in terms of sub-50 fs pulse generation at reasonable average output powers. Moreover, one can expect the generation of sub-20 fs pulses from this compound based on pure KLM.

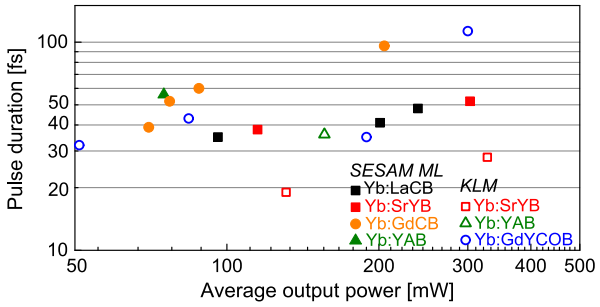

Fig. 8. Pulse duration vs. average output power of 1-µm passively mode-locked lasers based on various Yb^{3+}-doped borate crystals employing a similar laser architecture to that reported in the present work.

4. Conclusion

In summary, we have demonstrated, for the first time to our knowledge, mode-locked operation of a Yb:LaCB laser pumped by a spatially single-mode, fiber-coupled laser diode. Employing a SESAM to initiate and stabilize ML operation, we successfully generated soliton pulses as short as 35 fs with a central wavelength of 1055.9 nm. By utilizing a 7.5% OC, the average output power was scaled up to 239 mW, corresponding to a peak power of 65.9 kW and a laser efficiency of 29%. These results underscore the promising potential of the Yb:LaCB crystal as a gain medium for generating ultrashort pulses approaching the few-optical-cycle regime.

Funding. National Natural Science Foundation of China (62475263); Science and Technology Projects of Fujian Province (2024I0041, 2023H0047); Sino-German Scientist Cooperation and Exchanges Mobility Program (M-0040); Ministerio de Ciencia, Innovación y Universidades (PID2022-141499OB-I00).

Acknowledgment. Xavier Mateos acknowledges the Serra Húnter program.

Disclosures. The authors declare no conflicts of interest.

Data availability. Data underlying the results presented in this paper are not publicly available at this time but may be obtained from the authors upon reasonable request.

References

1. L. Gudzenko, M. Kosmyna, A. Shekhovtsov, *et al.*, "Crystal growth and glass-like thermal conductivity of $Ca_3RE_2(BO_3)_4$ (RE = Y, Gd, Nd) single crystals," Crystals **7**(3), 88 (2017).
2. J. Álvarez-Pérez, J. Cano-Torres, A. Ruiz, *et al.*, "A roadmap for laser optimization of Yb:$Ca_3(NbGa)_5O_{12}$-CNGG-type single crystal garnets," J. Mater. Chem. C **9**(13), 4628–4642 (2021).
3. M. Serrano, J. O. Álvarez-Pérez, C. Zaldo, *et al.*, "Design of Yb^{3+} optical bandwidths by crystallographic modification of disordered calcium niobium gallium laser garnets," J. Mater. Chem. C **5**(44), 11481–11495 (2017).
4. A. Yoshida, A. Schmidt, V. Petrov, *et al.*, "Diode-pumped mode-locked Yb:YCOB laser generating 35 fs pulses," Opt. Lett. **36**(22), 4425–4427 (2011).
5. F. Druon, F. Balembois, P. Georges, *et al.*, "Generation of 90-fs pulses from a mode-locked diode-pumped Yb^{3+}:$Ca_4GdO(BO_3)_3$ laser," Opt. Lett. **25**(6), 423–425 (2000).
6. F. Druon, S. Chenais, P. Raybaut, *et al.*, "Diode-pumped Yb:$Sr_3Y(BO_3)_3$ femtosecond laser," Opt. Lett. **27**(3), 197–199 (2002).
7. C. Tu, Y. Wang, Z. You, *et al.*, "Growth and spectroscopic characteristics of $Ca_3Gd_2(BO_3)_4$:Yb^{3+} laser crystal," J. Cryst. Growth **265**(1-2), 154–158 (2004).
8. A. Brenier, C. Tu, Y. Wang, *et al.*, "Diode-pumped laser operation of Yb^{3+}-doped $Y_2Ca_3B_4O_{12}$ crystal," J. Appl. Phys. **104**(1), 013102 (2008).

Optics EXPRESS

9. Y. Wang, Y. Wang, C. Sun, *et al.*, "Growth, spectroscopic characteristics and laser potential of Yb^{3+}:$Ca_3La_2(BO_3)_4$ crystal," Laser Phys. **22**(6), 1021–1028 (2012).
10. B. Mill, A. Tkachuk, E. Belokoneva, *et al.*, "Spectroscopic studies of $Ln_2Ca_3B_4O_{12}$-Nd^{3+} (Ln = Y, La, Gd) crystals," J. Alloys Compd. **275-277**, 291–294 (1998).
11. P. H. Haumesser, R. Gaumé, J. M. Benitez, *et al.*, "Czochralski growth of six Yb-doped double borate and silicate laser materials," J. Cryst. Growth **233**(1-2), 233–242 (2001).
12. J. L. Xu, J. He, H. Huang, *et al.*, "Performance of diode pumped Yb:$Y_2Ca_3B_4O_{12}$ laser with V^{3+}:YAG as saturable absorber for passively Q-switched mode-locking operation," Laser Phys. Lett. **7**(3), 198–202 (2010).
13. J. L. Xu, J. L. He, H. T. Huang, *et al.*, "Generation of 244-fs pulse at 1044.7 nm by a diode-pumped mode-locked Yb:$Y_2Ca_3(BO_3)_4$ laser," Laser Phys. Lett. **8**(1), 24–27 (2011).
14. Z. Pan, Z. L. Lin, P. Loiko, *et al.*, "Polarized spectroscopy and diode-pumped laser operation of disordered Yb:$Ca_3Gd_2(BO_3)_4$ crystal," Opt. Mater. Express **12**(2), 673–684 (2022).
15. H. J. Zeng, Z. L. Lin, W. Z. Xue, *et al.*, "Soliton mode-locked Yb:$Ca_3Gd_2(BO_3)_4$ laser," Opt. Express **30**(7), 11833–11839 (2022).
16. L. Wang, H. Xu, Z. Pan, *et al.*, "Anisotropic laser properties of Yb:$Ca_3La_2(BO_3)_4$ disordered crystal," Opt. Mater. **58**, 196–202 (2016).
17. Z. Pan, H. Cai, H. Huang, *et al.*, "Growth, thermal properties and laser operation of a novel disordered Yb:$Ca_3La_2(BO_3)_4$ laser crystal," Opt. Mater. **36**(12), 2039–2043 (2014).
18. Y. Wang, A. Chen, and C. Tu, "Comparison of actively Q-switched laser performance of disordered Yb:$Ca_3La_2(BO_3)_4$ crystals cut along the crystallographic axes," Appl. Opt. **54**(8), 2066–2071 (2015).
19. Y. Wang, A. Chen, Z. You, *et al.*, "Polarized spectra calculation and continuous wave laser operation of Yb-doped disordered $Ca_3La_2(BO_3)_4$ crystal," Laser Phys. **25**(12), 125801 (2015).
20. L. Wang, W. Han, Z. Pan, *et al.*, "High-energy passively Q-switched laser operation of Yb:$Ca_3La_2(BO_3)_4$ disordered crystal," Appl. Opt. **55**(13), 3447–3451 (2016).
21. J. A. Caird, S. A. Payne, P. Staber, *et al.*, "Quantum electronic properties of the $Na_3Ga_2Li_3F_{12}$:Cr^{3+} laser," IEEE J. Quantum Electron. **24**(6), 1077–1099 (1988).